First publ. in: Laser Physics 7 (1997), 2, pp. 343-348

Study of Nucleation Processes during Laser Cleaning of Surfaces

O. Yavaş, A. Schilling, J. Bischof, J. Boneberg, and P. Leiderer

Fakultät für Physik, Universität Konstanz, Postfach 5560 M767, Konstanz, D-78434 Germany

e-mail. Paul.Leiderer@uni-konstanz.de

Received September 18, 1996

Abstract—Bubble nucleation and growth dynamics on a nanosecond time scale induced by pulsed laser heating or acoustic cavitation are studied experimentally. Sensitive test methods such as optical reflection and light scattering, piezoelectric transducer, and surface plasmons are used to monitor threshold fluences for bubble nucleation, bubble growth velocities, and pressure effects in various liquids. A long-term memory effect, i.e., enhanced acoustic cavitation following laser-induced bubble formation at a liquid–solid interface could be demonstrated and its decay mode determined. Recent experimental results show that surface plasmons are especially sensitive for the study of the early stages of bubble nucleation, indicating that bubble nucleation sets on at a lower liquid superheat than previously determined using optical reflectance or piezoelectric transducer methods.

1. INTRODUCTION

One of the challenging tasks in the microelectronic fabrication process impeding further development in chip miniaturization is the removal of submicroscopic particle contaminants from solid surfaces without damaging the surface. Due to strong adhesion forces exerted with decreasing particle dimension, the conventional cleaning methods, such as ultrasonics, are inefficient for the removal of submicroscopic particles and cause significant yield losses in the manufacturing process [1, 2]. Recently, it has been demonstrated that submicroscopic particles down to 0.2 μm can efficiently be removed by steam laser cleaning [3–5]. In this laser-cleaning process that motivated the present work, a thin liquid film is deposited onto the contaminated surface, which is rapidly heated by pulsed laser irradiation. The subsequent explosive evaporation of the liquid film causes the removal of the contaminating particles.

The explosive evaporation of liquids induced by short-pulsed laser irradiation is also of importance in a variety of technological applications in medicine and industry, such as laser surgery, laser chemistry, localized depassivation of metallic surfaces, and phase-conjugate mirror design [6–9]. It is further of interest for the understanding of metastability behavior of superheated liquids, which is well established only in the near-steady-state regime on a time scale of microseconds or longer, because traditional experimental techniques, such as short-pulsed electrical current heating, lack speed and sensitivity [10]. The application of pulsed laser heating enables the study of phase transitions on much shorter time scales. Indeed, we have recently been able to study the nucleation and growth dynamics of bubbles at a liquid–solid interface induced by nanosecond-pulsed laser heating using various test methods, such as optical reflectance, light-scattering, and piezoelectric transducer measurements [11, 12].

Similarly, acoustic cavitation, i.e., the formation of bubbles or cavities in a liquid induced by the tensile pressure of an acoustic field, is of importance for a better understanding of liquid–vapor phase-change phenomena and is widely applied in technical processes, such as sonochemistry, ultrasonic cleaning, and shock-wave lithotripsy [13, 14]. The time scale for previous studies on acoustic cavitation had been limited to microseconds due to the inability of transducers to generate shorter acoustic pulses of sufficient intensities. However, we have recently demonstrated the generation of acoustic cavitation by nanosecond pulses and the existence of a bubble memory effect at a liquid–solid interface [15, 16].

Here, we will first give a brief survey of our previous studies on the bubble nucleation and growth dynamics and cavitation phenomena on a nanosecond time scale. Afterwards, we will present our recent experiments using surface plasmons to study the early stages of bubble nucleation at a liquid–solid interface induced by pulsed laser heating. Due to its higher sensitivity for smaller bubbles, this novel method enables the determination of nucleation thresholds with considerably higher accuracy than the previous probe methods.

2. OPTICAL REFLECTANCE AND PIEZOELECTRIC TRANSDUCER STUDIES

2.1. Experimental Apparatus and Procedure

In the laser-cleaning process, the liquid film evaporation is accompanied by strong droplet ejection and film rupture, which complicates the study of the transient nucleation phenomena on a solid surface [17]. To eliminate the undesired "thin film" effects, experiments have been performed using bulk liquids in contact with solids in the absence of liquid-free surfaces. The experimental setup is shown in Fig. 1. A test liquid is contained in a cuvette made of fused quartz and the solid

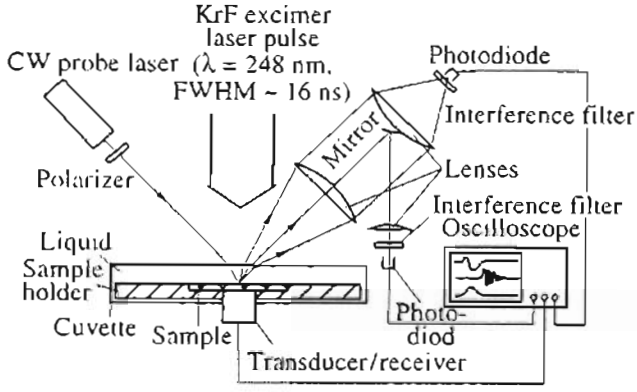

Fig. 1. Experimental configuration for the nanosecond time-resolved study of laser-induced bubble formation at a liquid–solid interface using optical reflectance, light-scattering and piezoelectric-transducer probes.

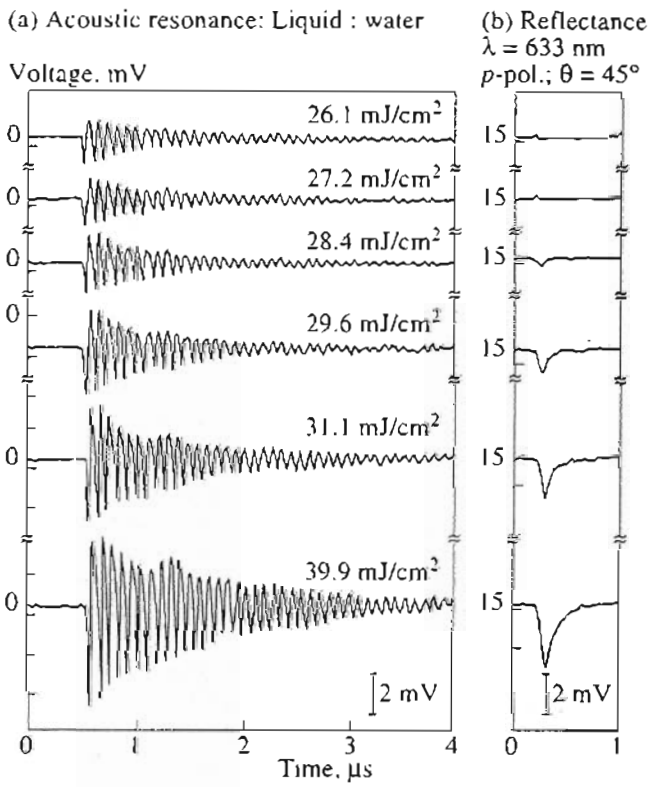

Fig. 2. Simultaneously acquired acoustic and optical signals for water–chromium interface with increasing excimer laser fluence.

sample is mounted on a massive stainless steel block immersed entirely into the liquid. A 248-nm KrF excimer laser pulse (FWHM = 16 ns) is directed at normal incidence onto the sample, irradiating a relatively large area (1 × 1 cm²). A low-power cw laser probe beam is focused into the center of the excimer laser irradiated area at oblique incidence. Optical reflectance, light-scattering, and acoustic signals can be detected simultaneously by fast photodetectors (rise time < 1 ns) and by a piezoelectric transducer (bandwidth 20 MHz). All the signals are monitored on a digital storage oscilloscope triggered by the excimer laser pulse. The test liquids studied are pure water, IPA (isoprophyl alcohol), ethanol, methanol, and mixtures of water and IPA, which are transparent to the KrF excimer laser beam. A 0.2-μm-thick chromium film was used as the absorbing solid because of its thermal stability and the expected insensitivity of its optical properties to temperature changes (see the next section). The angle of incidence for the probe beam was varied between 7° and 45°. Its polarization was either normal to the plane of incidence (*s*-polarization) or parallel to the plane of incidence (*p*-polarization). By position-sensing experiments using a knife edge and a bicell, it has been verified that there is no measurable contribution to the reflectance signal due to any probe beam deflection. Accordingly, any change on the reflectance signal could be ascribed to nucleation and growth of bubbles at the liquid–solid interface.

2.2. *Experimental Results*

The experiment was first conducted by applying excimer laser fluences up to 100 mJ/cm² to the bare chromium surface in the absence of liquid. No change in the optical signal was observed, indicating that the optical properties of the chromium film are temperature-independent in the present temperature range. When the experiment was conducted with liquid in the cuvette, the reflectance signal exhibited distinct transients above a liquid-dependent threshold fluence. Figure 2 shows one set of the transient optical reflectance and acoustic transducer signals with increasing laser fluence for a water–chromium interface, where the probe beam of 633 nm was *p*-polarized and incident at an angle of 45°. Similar transients with minor differences were obtained for all the investigated liquids.

The threshold fluence for bubble nucleation (more strictly speaking, the threshold for bubble growth up to a size comparable to probe wavelength as will be discussed in the next section) could be accurately determined by plotting the amplitude of the reflectance drop or the acoustic signal amplitude as a function of the excimer laser fluence. The resulting graphs are shown in Fig. 3. There is a liquid-dependent threshold fluence above which the reflectance signal suddenly starts to drop. The interception of the plot with the *x*-axis has been interpreted as the threshold fluence for bubble nucleation [11, 12]. Similarly, the acoustic signal amplitude exhibits a sudden increase due to bubble nucleation. As expected, the threshold fluence for bubble nucleation in water is higher than that for bubble nucleation in alcohols or water–alcohol mixtures. The temperature at the liquid-solid interface has been computed using the finite element method for the experimentally observed threshold fluence for the liquids under study. The computations reveal that nucleation takes place when the liquids are only moderately super-

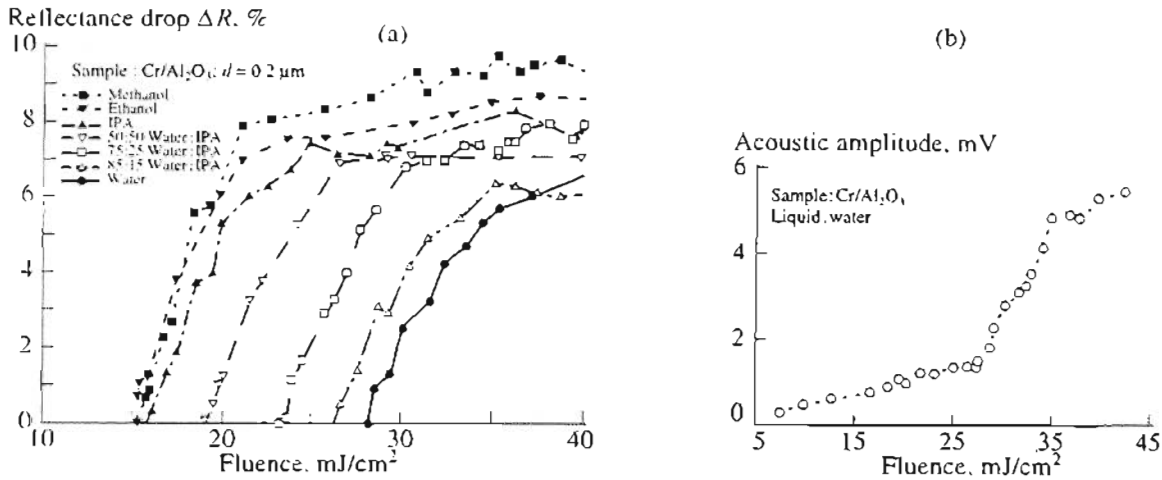

Fig. 3. Threshold behavior of (a) acoustic and (b) optical signals.

heated (for example, ethanol 24 K and water 53 K), which is in agreement with the well-known fact that heterogeneous nucleation of bubbles is strongly affected by surface roughness and texture because microcavities and crevices provide active sites for embryonic bubbles [18]. It has been verified recently that the results of the computations agree well with the experimentally obtained temperature at the sample surface [19].

The shape of the reflectance signal depends on the angle of incidence and the polarization of the probe laser beam. When the angle of incidence is small (<40°), the same shape for the optical reflectance signal is observed for both the *s*- and the *p*-polarized probe beam: an abrupt increase is followed by a more gradual dip. When the angle of incidence exceeds 40°, however, the leading positive part of the signal is only observable for the *s*-polarized probe beam. An example of this behavior is depicted in Fig. 4. The simultaneously measured scattering signal demonstrates that the observed transient decrease in the optical reflectance signal is caused by the scattering of the probe beam from vapor bubbles. Using an effective medium theory by Maxwell Garnett [20], it could further be demonstrated that the initial peak in the optical reflectance signal is due to small bubbles (i.e., $R \ll \lambda_{probe}/2\pi n_{liq}$, where R is the bubble radius and n_{liq} is the refractive index of the liquid) uniformly distributed at the liquid–solid interface [11, 12]. When the bubbles grow in size ($R \gg \lambda_{probe}/2\pi n_{liq}$), light scattering dominates, resulting in a decrease of the reflectance signal. In order to determine the bubble growth velocities, we used the facts that the transition radius depends on the probe beam wavelength as $R \approx \lambda_{probe}/2\pi n_{liq}$, and that in the initial inertia-controlled stage bubble radius increases linearly with time [18]. On this basis, bubble growth velocities for different liquids could be estimated from the width of the initial peak in the reflectance signal and were found to be on the order of m/s ($v \approx 2$–2 and 4 m/s for alcohols and water, respectively) [11, 12]. Recent interferometric measurements by Park *et al.* [21] provide bubble growth velocities of the same order, confirming our results.

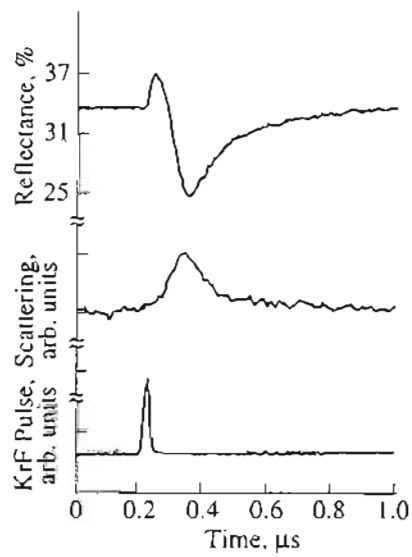

Fig. 4. Simultaneously acquired optical reflectance and light-scattering signals for isopropanol–chromium interface (λ_{probe} = 633 nm, unpolarized, θ = 20°), demonstrating that the reflectance drop is caused by scattering losses on laser-induced bubbles.

When the heat deposited at the liquid–solid interface diffuses out, the thermally induced bubbles collapse within a few hundred nanoseconds. Accordingly, the optical reflectance signal returns to the initial level. However, the acoustic pulse generated by the nucleation process that propagates in the liquid is reflected back to the sample at the quartz window, and causes cavitation at the liquid–solid interface after its round trip in the cuvette. As a result, on a longer time scale, repetitive "echoes" in the optical reflectance signal are observed when the surfaces of the solid sample and the

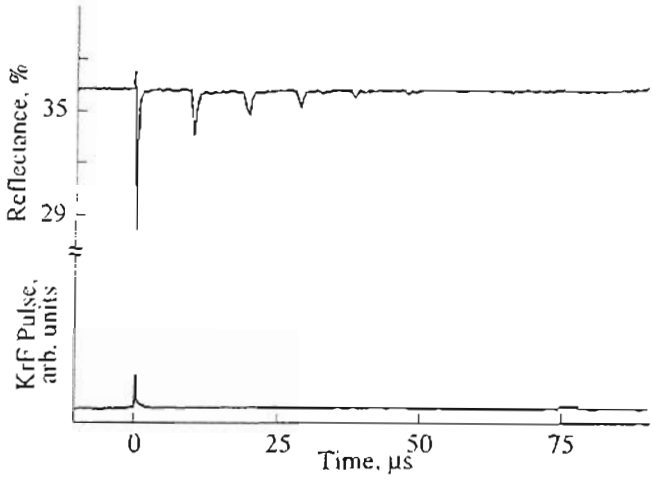

Fig. 5. Repetitive "echoes" in the optical reflectance signal in the microsecond time scale, indicating the existence of a long-term memory effect for acoustic cavitation.

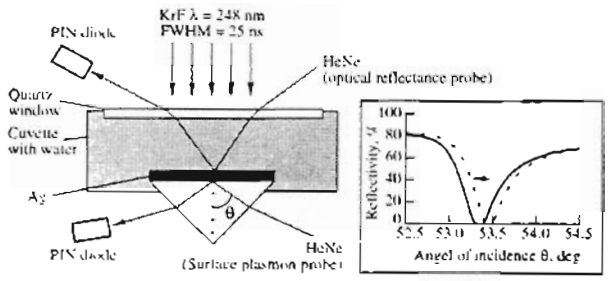

Fig. 6. Experimental setup for the time-resolved study of laser-induced bubble nucleation phenomena at a liquid–solid interface using surface plasmon and optical reflectance probes. Inset shows the expected shift of the surface plasmon resonance curve to smaller angles due to bubble formation at the liquid–solid interface.

quartz window are parallel to each other so that the acoustic pulse is reflected back and forth. As shown in Fig. 5, the amplitude of these echo signals decreases successively, which is partly due to the attenuation of the acoustic wave by absorption and to reflection losses. However, by tilting the quartz window with respect to the sample surface and thus probing different areas of the sample surface, we have proven that preceding thermally induced bubble formation at the liquid–solid interface is an essential requirement for the observed acoustic cavitation [15, 16]. A possible explanation for this "memory effect" is that the thermally induced bubbles do not completely disappear when they collapse, but survive for a few hundreds of microseconds, serve as embryonic bubbles, and enhance acoustic cavitation.

In view of these unsolved problems, and considering the fact that the previously used ORP technique detects the bubbles first when they reach a certain size comparable to the probe beam wavelength, a new test method is required which is sensitive to bubbles much smaller than the probe beam wavelength and can provide information also at the early stages of the nucleation process. Therefore, we have applied the surface plasmon probe as a sensitive tool for the study of nucleation processes at a liquid–solid interface.

3. SURFACE PLASMON PROBE STUDIES

3.1. Experimental Setup and Procedure

The experimental setup for the surface plasmon probe (SPP) of the laser-induced bubble nucleation at a liquid–solid interface is depicted in Fig. 6. A thin silver film of 53 nm is evaporated in high vacuum onto the base of a heavy flint glass prism ($n = 1.7494$ for $\lambda = 632.8$ nm). A 2-nm thick chromium interlayer is used to increase the adhesion between the silver film and the glass prism. The prism with the silver film is mounted on a cuvette filled with distilled water. Surface plasmons are excited optically at the silver–water interface via attenuated total reflection (ATR) in the Kretschmann configuration using a 5-mW HeNe probe laser [22]. Bubble nucleation occurs at the silver–water interface upon heating by a KrF excimer laser pulse ($\lambda = 248$ nm, FWHM ≈ 25 ns, spot size 1 × 1 cm) through a quartz window. Any transient change of the surface plasmon resonance angle due to a change of the dielectric function of the water layer on the silver film caused by bubble nucleation, temperature rise, or pressure changes is monitored using a fast photodiode (rise time < 1 ns), whose signal is amplified using an ac-coupled 1 GHz bandwidth amplifier, and recorded on a 500-MHz digitizing storage oscilloscope. As indicated in the inset of Fig. 6, it is expected that the bubble nucleation will cause a shift of the surface plasmon resonance to a smaller angle of incidence, since the effective dielectric function of the water layer adjacent to the silver film will decrease when bubbles are formed. With the help of a second HeNe probe laser, incident from the front side through the liquid and probing the same spot as the SPP, transient reflectance changes due to light scattering caused by grown-up bubbles could be measured simultaneously. The measurements presented in the following have been performed by setting the angle of incidence of the probe beam to the middle of the left wing of the surface plasmon resonance, as indicated by the arrow in the inset of Fig. 6.

3.2. Experimental Results and Discussion

As already mentioned, the position and shape of the plasmon resonance are influenced by several effects. In order to determine first the contribution of the temperature rise in the silver film, experiments have been conducted with the bare silver film in the absence of water. Due to combined effects of plasmon resonance shift and broadening, the temporal shape of the probe signal depends on the angle of incidence for the probe beam. A thorough discussion of this behavior is given

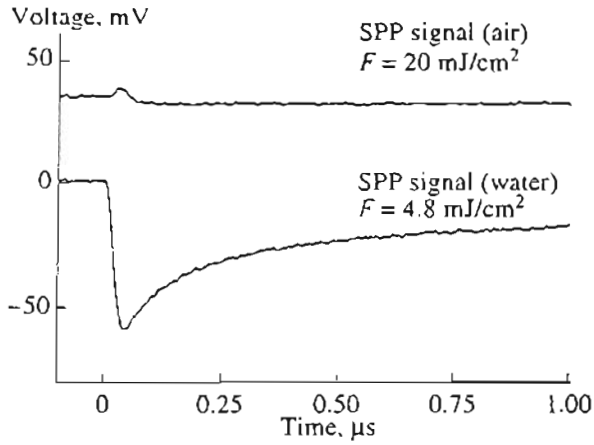

Fig. 7. Comparison of surface plasmon probe signals acquired without (top curve) and with the presence of water (bottom curve) in the cuvette. 10 mV corresponds to a reflectance change of 3%. The curves are offset for clarity.

by Herminghaus and Leiderer [23]. The observed reflectance changes are relatively small, being about 3% for the highest laser fluence used, $F = 32$ mJ/cm^2, for which numerical computations yield a peak temperature of $T = 746$ K in the silver film. The temporal decay of the reflectance drop is governed by the sudden temperature rise in the silver film due to rapid laser heating in a few nanoseconds and the subsequent gradual decrease of the temperature due to heat transfer on a microsecond time scale.

The amplitude of the reflectance drop is drastically increased, when the experiment is conducted with the cuvette filled with water. The change of the optical properties of the dielectric half-space (in our case water) due to a given temperature rise [24] causes a much larger shift of the surface plasmon resonance than a change of the optical properties of the silver film [25] induced by the same temperature rise. Consequently, the resulting shape of the SPP is predominantly governed by the changes of the refractive index of water with temperature. A comparison of transient SPP signals acquired without and with water is given in Fig. 7. Note that in the presence of water the observed reflectance change amounts to 18%, which, despite the 5 times lower laser fluence used, is 6 times higher compared to the case of laser irradiation of the bare silver surface. As expected, a transient decrease in the SPP signal is observed, due to a shift of the surface plasmon resonance to smaller angles with increasing temperature. As long as the laser fluence is below a certain threshold (which corresponds to the threshold for bubble nucleation, see below), the SPP signal exhibits no particular extra features.

When the excimer laser fluence is increased further, however, an additional structure in the SPP signal is observed, as shown in Fig. 8. A hump in the reflectance drop starts to appear at an excimer laser fluence of F = 9.5 mJ/cm^2 and is more pronounced with increasing

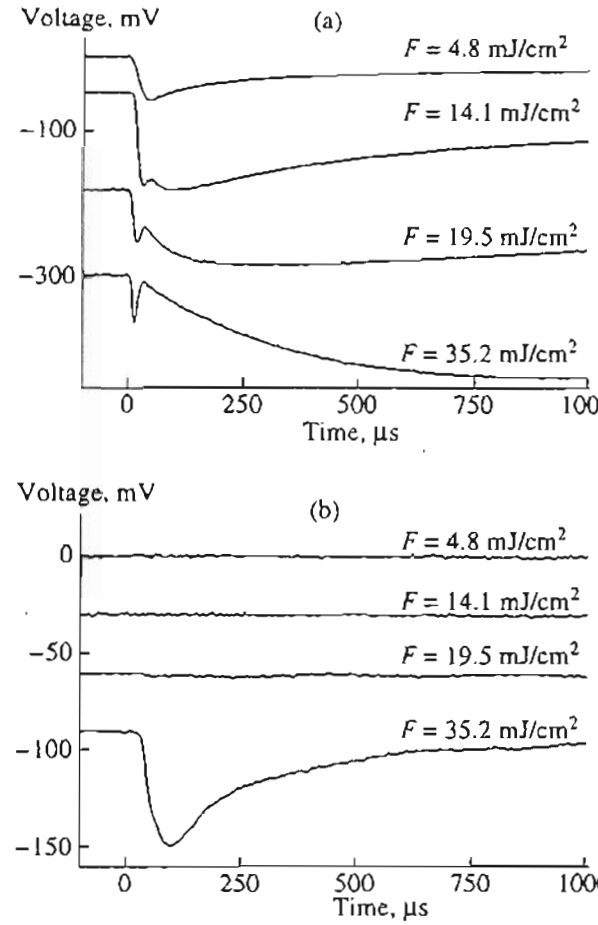

Fig. 8. (a) Surface plasmon probe and (b) optical reflectance signals for water–silver interface with increasing excimer laser fluence. 10 mV corresponds to a reflectance change of 3%. The curves are offset for clarity.

laser fluence. The appearance of this hump can be interpreted as the onset of bubble nucleation at the water–silver interface: The surface plasmons are effectively scattered by the bubbles, and, consequently, the surface plasmon resonance is broadened, resulting in a temporary increase of the reflectance. When the bubbles collapse, the surface plasmon resonance becomes again narrower and the reflectance decreases to a level which is given by the resonance shift due to the actual temperature present at the liquid–solid interface. For the laser fluence of $F = 10.5$ mJ/cm^2, numerical computations yield a peak temperature of $T = 384$ K at the liquid–solid interface, i.e., a liquid superheat of $T = 12$ K. For comparison, the threshold fluence for the same system determined simultaneously using an optical reflectance probe (ORP) is $F = 19.5$ mJ/cm^2, which corresponds to a peak temperature of $T = 473$ K at the liquid–solid interface (superheat, $T = 101$ K). This result strikingly demonstrates the high sensitivity of surface plasmon probe to small bubbles which collapse before they grow up to the order of the probe beam wavelength and therefore remain invisible to the ORP. It has been previously

pointed out that the thickness of the superheated liquid layer is a limiting factor for the maximum bubble size achievable [26]. The difference in the threshold fluences acquired using these two different methods can be explained by assuming that the threshold temperature obtained using the SPP corresponds to the temperature where the bubble nucleation sets in, and the threshold temperature obtained using the ORP corresponds to the temperature where the bubble growth becomes effective. Recently, we have successfully demonstrated that, in addition to the detection of submicroscopic bubbles, the surface plasmon probe can be used also for absolute pressure measurements on the nanosecond time scale with a sensitivity of about 1 bar [27].

4. CONCLUSIONS

A variety of aspects of bubble nucleation and growth dynamics on a nanosecond time scale induced by pulsed laser heating and acoustic cavitation have been studied experimentally. The threshold fluences for bubble nucleation and growth have been determined accurately. The bubble growth velocities have been estimated to be on the order of m/s. A long-term memory effect for acoustic cavitation has been demonstrated and its decay mode in a few hundred microseconds has been determined. In particular, the surface plasmon probe proved to be a sensitive tool for the study of the early stages of bubble nucleation. It turns out that a liquid superheat as low as 11 K can lead to bubble nucleation at a water–silver interface. However, in order to induce effective bubble growth up to the order of the probe beam wavelength, a liquid superheat of about 100 K is required. Otherwise, the bubbles collapse and disappear. These embryonic bubbles, which remain invisible to the optical reflectance probe due to the lack of effective light scattering, could be detected by the surface plasmon probe due to its higher sensitivity to changes of refractive index at the liquid–solid interface. Further work using the surface plasmon probe is in progress in order to study the effect of the surface conditions of the silver film on the nucleation behavior and the pressure effects involved in the nucleation process.

ACKNOWLEDGMENTS

This work was supported by the Center of Modern Optics at the University of Konstanz, Germany.

REFERENCES

1. Hoenig, S.A., 1988, *Particles on Surfaces*, Mittal, K.L., Ed. (New York: Plenum), 1, 3.
2. Hattori, T., 1990, *Solid State Tech.*, 8, July.
3. Zapka, W., Ziemlich, W., and Tam, A.C., 1991, *Appl. Phys. Lett.*, **58**, 2217.
4. Tam, A.C., Leung, W.P., Zapka, W., and Ziemlich, W., 1992, *J. Appl. Phys.*, **71**, 3515.
5. Park, H.K., Grigoropolous, C.P., Leung, W.P., and Tam, A.C., 1994, *IEEE Trans. Comp., Pack., and Manuf. Tech. A*, **17**, 631.
6. Parrisch, J.A. and Deutsch, T.F., 1984, *IEEE J. Quantum Electron*, **20**, 1386.
7. Bäuerle, D., 1996, *Chemical Processing with Lasers* (Berlin: Springer).
8. Oltra, R., Indrianjafy, G.M., and Boquillon, J.P., 1991, *J. Phys. C IV*, **7**, 769.
9. Jones, D.C., Mangir, M.S., and Rockwell, D.A., 1996, *Opt. Commun*, **123**, 175.
10. Skripov, V.P., 1974, *Metastable Liquids* (New York: Wiley).
11. Yavaş, O., Leiderer, P., Park, H.K., *et al.*, 1993, *Phys. Rev. Lett.*, **70**, 1830.
12. Yavaş, O., Leiderer, P., Park, H.K., *et al.*, 1994, *Appl. Phys. A*, **58**, 407.
13. Mason, T.J., 1991, *Practical Sonochemistry* (New York: Ellis Horwood).
14. Watson, G.M., Jacques, S.L., Dretler, S.P., and Parrish, J.A., 1985, *Lasers Surg. Med.*, **5**, 160.
15. Yavaş, O., Leiderer, P., Park, H.K., *et al.*, 1994, *Phys. Rev. Lett.*, **72**, 2021.
16. Yavaş, O., 1994, *Laserinduzierte Gasblasennukleation*, (Konstanz: Hartung-Gorre).
17. Leung, P.T., Do, N., Klees, L., *et al.*, 1992, *J. Appl. Phys.*, **72**, 2256.
18. Carey, V.P., 1992, *Liquid–Vapor Phase-Change Phenomena* (Washington: Hemisphere).
19. Park, H.K., Grigoropolous, C.P., Poon, C.C., and Tam, A.C., 1996, *Appl. Phys. Lett.*, **68**, 596.
20. Maxwell Garnett, J.C., 1904, *Phil. Trans. Roy. Soc. London*, **203**, 385.
21. Park, H.K., Grigoropoulos, C.P., Poon, C.C., and Tam, A.C., to be published.
22. Kretschmann, E. and Raether, H., 1968, *Z. Naturf. A*, **23**, 2135.
23. Herminghaus, S. and Leiderer, P., 1990, *Appl. Phys. A*, **51**, 350.
24. Schiebener, P., Straub, J., Levelt Sengers, J.M.H., and Gallagher, J.S., 1990, *J. Phys. Chem. Ref. Data*, **19**, 677.
25. Johnson, P.B. and Christy, R.W., 1972, *Phys. Rev. B*, **6**, 4370.
26. Park, H.K., 1994, Heat and Momentum Transfer on the Rapid Phase Change of Liquid Induced by Nanosecond-Pulsed Laser Irradiation, *Dissertation* (Univ. of California at Berkeley).
27. Schilling, A., Yavaş, O., Bischof, J., *et al.*, submitted for publication in *Appl. Phys. Lett.*